

# Analysis of a phase shifter based on a slot polymeric waveguide with liquid crystal cladding

Flavio Cornaggia, Badrul Alam, Antonio d'Alessandro, and Rita Asquini

Department of Information Engineering, Electronics and Telecommunications, "Sapienza" University of Rome, Rome, Italy  
e-mail: [rita.asquini@uniroma1.it](mailto:rita.asquini@uniroma1.it)

**Abstract**—We numerically investigated a phase shifter based on a polymeric platform by using two different approaches. The device consists of a polymeric slot waveguide covered with an organic liquid crystal cladding, which is a promising configuration for the implementation of polymeric waveguide systems for computation, communication and sensing. Two different nematic liquid crystals have been considered, E7 and 5CB. At first, we have indirectly computed the phase shift through a combination of 2D Finite Element Method with index ellipsoid theory. Then, we have investigated the signal propagation by means of 3D Finite Difference Time Domain Method, which allowed to obtain also the intrinsic propagation loss of the structure and the materials. Although each approach introduces specific approximations and requires different resources, both give similar results and confirm the excellent quality of the device, namely low propagation losses and relevant phase shifting capability.

**Keywords**—Optical integrated circuits, FDTD, FEM, liquid crystal, waveguide, phase shift.

## I. INTRODUCTION

Phase shifting is a key operation in many optical devices and systems. It can be implemented in optical integrated circuits with low propagation losses, fast response times and high integration density [1,2,3,4]. One mechanism to induce a phase shift takes advantage of the electro-optical effect through materials such as liquid crystals (LC) [5].

LCs are interesting materials for developing low-power photonic devices, thanks to their large electro-optic response and nonlinear optical properties. Their high birefringence can be exploited to reorient their molecules through electric [6] or optical [7] fields. Moreover, when used as cladding [8,9,10], LCs show remarkable switching and tuning capabilities with low voltage and low propagation losses. The integration of LC cells proved to be compatible with both semiconductor and polymeric waveguiding systems. Moreover, when combined with LC, polymer-based optical integrated circuits can greatly boost performances and add new functionalities in sensing, computation, and communications [11,12]. Therefore, it is very important to define new methods to study switching capabilities of these technologies and to evaluate them.

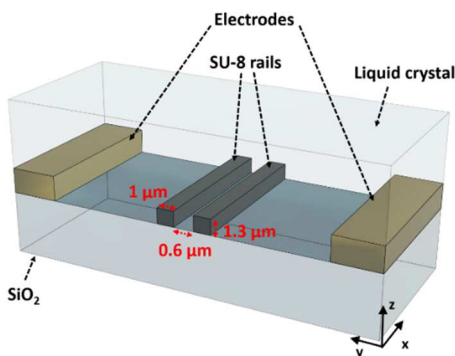


Figure 1. Cross section of the optical phase shifter under analysis.

In this work, we analyze light propagation, transmission losses and achievable maximum phase shift in a polymeric slot waveguide with a liquid crystal cladding, by approaching the study in two different ways. At first, we indirectly investigate the system, through a two dimensional Finite Element Method (2D-FEM) combined with index ellipsoid theory [5]. Then we directly study the waveguide behavior in a small section by using a three dimensional Finite Difference Time Domain (3D-FDTD) method. The results of the two analyses applied to two types of nematic LCs (5CB and E7) are discussed and compared.

## II. OPTICAL STRUCTURE AND WORKING PRINCIPLE

The device is designed to work at 1.55- $\mu\text{m}$  wavelength with TE mode. Figure 1 shows the device cross section. It consists in a slot waveguide obtained through two rails of SU-8 2000 ( $n = 1.573$ ), with an upper anisotropic cladding made of LC and built upon a SiO<sub>2</sub> substrate ( $n = 1.4657$ ). We investigated both LCs E7 (ordinary refractive index  $n_o = 1.5$ , extraordinary refractive index  $n_e = 1.689$ ,  $\Delta n = 0.189$ ) and 5CB ( $n_o = 1.511$ ,  $n_e = 1.678$ ,  $\Delta n = 0.167$ ). We chose a planar configuration for electrodes, spaced by 20  $\mu\text{m}$ . The waveguide is optimized to support only TE-like<sub>00</sub> and TM-like<sub>00</sub> modes. The rails are 1.3- $\mu\text{m}$  high and 1- $\mu\text{m}$  wide, at 0.6  $\mu\text{m}$  distance between them (slot gap).

When no voltage is applied, the LC molecules align towards the waveguides longitudinal direction ( $x$  axis in Figure 1). Then, a voltage between the electrodes induces a reorientation of the LC molecules toward the applied electric field: hence, the LC twists on the  $xy$  plane (see Figure 1). Since the electric field affects the refractive index experienced by the TE<sub>00</sub> mode, which depends on the final angle, then a phase shift is introduced along the waveguide.

## III. FEM ANALYSIS

By extensively using the mode solver from 2D FEM, and leveraging on software conformal meshing, we have first modeled the slot waveguide and then, indirectly, we have computed the phase shift by combining simulation results with index ellipsoid theory. Given the molecules twist on the  $xy$  circuit plane, the LC refractive index is [5]:

$$n_e(\theta) = \frac{n_e n_o}{\sqrt{n_e^2 \cos^2(\theta) + n_o^2 \sin^2(\theta)}} \quad (1)$$

where  $n_o$  is the ordinary index,  $n_e$  is the extraordinary index, and  $\theta$  is the twist angle (from axis  $x$  to  $y$  in Figure 1). Moreover, since the main part of the mode field distribution is concentrated in a small area and given the large distance between electrodes, we have approximated the electric field direction as being parallel to the circuitual plane. In this way, the resulting index variations results as in isotropic media.

Given the relationship (1) between LC refractive index and twist angle, we separately evaluated middle values of  $n(\theta)$  between  $n_e$  and  $n_o$ . Then, we run various 2D-FEM simulations with isotropic upper cladding and the boundary conditions set to Perfectly Matched Layers (PML).

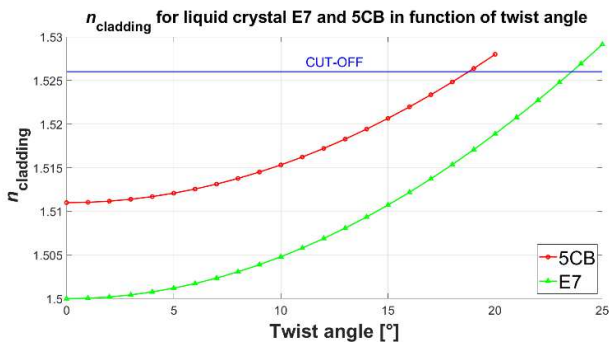


Figure 2: Cladding refractive index vs. twist angle.

Figure 2 shows that for a critical value  $n(\theta) = n_{co}$  the slot mode exceeds the cut-off level; in our situation,  $n_{co} \approx 1.526$ , corresponding to  $\theta = 24^\circ$  for E7 and  $\theta = 19^\circ$  for 5CB.

In order to evaluate the relative phase shift  $\Delta\varphi$  per length of the waveguide  $L$ , we used the classical relations:

$$\varphi = k \cdot L = \frac{2\pi}{\lambda} \cdot n_{eff} \cdot L \quad (2)$$

$$\begin{aligned} \Delta\varphi &= \Delta k \cdot L = \frac{2\pi}{\lambda} \cdot \Delta n_{eff} \cdot L \\ &= \frac{2\pi}{\lambda} \cdot (n_{eff}(\theta) - n_{eff(0)}) \cdot L \end{aligned}$$

where  $n_{eff}(\theta)$  is the effective index of the mode, whilst  $n_{eff(0)}$  is the one without excitation. In this way, for a 1-mm reference length we get:  $\Delta\varphi_{E7} = 20\pi$  and  $\Delta\varphi_{5CB} = 13\pi$ .

#### IV. FDTD ANALYSIS

While the previous approach was 2D, the FDTD analysis was carried out 3D, by using a cubic mesh approximation. In addition to phase shift, it was possible to compute also the intrinsic propagation loss and to take into account LC anisotropy. Given the high computational requirements, it was possible to compute the propagation only along a 20- $\mu\text{m}$  long waveguide. We computed the transmission loss in dB/cm by means of:

$$TL = 10 \log_{10} \left[ \frac{W_i}{W_t} \right] [dB] \quad (3)$$

where  $W_i$  and  $W_t$  are the powers at the input and output monitors, respectively. Table 1 shows the results for both E7 and 5CB LCs; as it can be seen, losses increase with the twist angle. The reason can be understood from Figure 3, which shows the field distributions in various cut planes and in two situations: LC with no applied voltage (images A and C) and LC close to cut-off (images B and D). In the latter situation, the mode becomes more evanescent and lossy.

For a 1-mm reference length, the results from 3D-FDTD are  $\Delta\varphi_{E7} = 18\pi$  and  $\Delta\varphi_{5CB} = 8\pi$ .

Table 1: Transmission losses for E7 and 5CB LCs.

Twist E7	dB/cm	Twist 5CB	dB/cm
0°	0.027	0°	0.4007
8°	0.1079	7°	0.7213
15°	0.4584	15°	3.9037
20°	4.5635	//	//

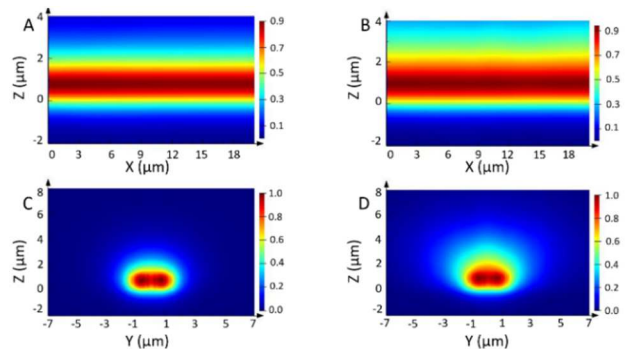


Figure 3: Device side views (A and B) and output transversal cut (C and D).

#### V. CONCLUSIONS

We demonstrated that both approaches, FEM and FDTD analysis, show high phase shifting efficiency of the device, which is comparable to the performances of semiconductor-based devices [9]. The less computationally demanding 2D-FEM study required the introduction of various approximations and could not estimate propagation losses. Instead, 3D-FDTD method allowed to compute all propagation parameters; despite its precision, it could simulate only a limited length of the device. The final results of the two approaches fairly match in values and in trend for the two considered LCs: this can be considered a mutual validation check. Overall, both methods can be employed, depending on available computational resources, capacity of meshing geometries, and desired precision.

#### REFERENCES

- [1] W. Bogaerts, et al., "Programmable photonic circuits", Nature 586, 207–216 (2020).
- [2] G. Calò, et al., "Dielectric and Plasmonic Vivaldi Antennas for On-chip Wireless Communications", 21st International Conference on Transparent Optical Networks (ICTON), Angers, France, pp. 1-4 (2019).
- [3] F. Fuschini, et al., "Multi-Level Analysis of On-Chip Optical Wireless Links", Appl. Sci. 10, pp. 196 (2020).
- [4] B. Alam, et al., "Numerical and Experimental Analysis of On-Chip Optical Wireless Links in Presence of Obstacles", IEEE Photonics Journal 13(1), pp. 1-11 (2021).
- [5] I.C. Khoo, "Liquid crystals", 2nd ed, Hoboken, Wiley; 2007.
- [6] R. Asquini, et al., "Electro-optic routing in a nematic liquid-crystal waveguide," Appl. Opt. 44(19), 4136-4143 (2005).
- [7] A. Piccardi, et al., "Trends and trade-offs in nematicon propagation", Appl. Phys. B: Lasers Optics., 104(4), pp. 805-811 (2011).
- [8] D. Donisi, et al., "Integration and characterization of LC/polymer gratings on glass and silicon platform", Mol. Cryst. Liq. Cryst. 516(1), pp. 152-158 (2010).
- [9] J. Pfeifle, et al., "Silicon-organic hybrid phase shifter based on a slot waveguide with a liquid-crystal cladding", Opt. Express 20, pp. 15359-15376 (2012).
- [10] G. Gilardi, et al., "All-optical and thermal tuning of a Bragg grating based on photosensitive composite structures containing liquid crystals", Mol. Cryst. Liq. Cryst. 558(1), pp. 64–71 (2012).
- [11] A. d'Alessandro, et al., "Polarization-independent nematic liquid crystal waveguides for optofluidic applications" IEEE Photon. Technol. Lett., 27(16), pp. 1709-1712 (2015).
- [12] A. Buzzin, et al., "On-Glass Integrated SU-8 Waveguide and Amorphous Silicon Photosensor for On-Chip Detection of Biomolecules: Feasibility Study on Hemoglobin Sensing", Sensors, 21(2), 415 (2021).